


ORIGINAL COMMUNICATION

Effects of shoulder abduction on the stiffness of supraspinatus muscle regions in rotator cuff tear

Yoshinari Sakaki^{1,2}  | Keigo Taniguchi² | Masaki Katayose² | Hideji Kura³ | Kenji Okamura³

¹Department of Rehabilitation, Hitsujigaoka Hospital, Sapporo, Japan

²Second Division of Physical Therapy, School of Health Sciences, Sapporo Medical University, Sapporo, Japan

³Department of Orthopaedic Surgery, Hitsujigaoka Hospital, Sapporo, Japan

Correspondence

Keigo Taniguchi, Second Division of Physical Therapy, School of Health Sciences, Sapporo Medical University, West 17, South 1, Chuo-ku, Sapporo, Hokkaido 060-8556, Japan.
Email: ktani@sapmed.ac.jp

Funding information

Japan Society for the Promotion of Science; Grant-in-Aid for Early Career Scientists, Grant/Award Number: 19K19833

Abstract

This study aimed to compare the effect of the load of the upper limb on the stiffness of supraspinatus muscle regions during isometric shoulder abduction in the scapular plane in healthy individuals and patients with a rotator cuff tear. Thirteen male patients were scheduled for arthroscopic rotator cuff repair, and 13 healthy male individuals were recruited. The movement task involved 30° isometric shoulder abduction in the scapular plane. The tasks included passive abduction, abduction with half-weight of the upper limb (1/2-weight), and full weight of the upper limb (full-weight). The stiffness of the supraspinatus muscle (anterior superficial, anterior deep, posterior superficial, and posterior deep regions) was recorded using ultrasound shear-wave elastography. The stiffness of the anterior superficial region on the affected side was significantly lower than that on the control side for the 1/2-weight and full-weight tasks. The stiffness of the anterior deep, posterior superficial, and posterior deep regions was not affected. This is the first study that investigated the mechanical effects of different loads on different supraspinatus muscle regions in rotator cuff tear patients. Our results indicate that the anterior superficial region in rotator cuff tear patients was mainly responsible for reduced active stiffness. This might be because this region contributes to force exertion and exhibits atrophy in rotator cuff tears. Hence, the anterior superficial region could be a focal point of quantitative dysfunction evaluation of the supraspinatus muscle in the case of a rotator cuff tear.

KEYWORDS

elastic modulus, elastography, rotator cuff tear, supraspinatus

1 | INTRODUCTION

A rotator cuff tear (RCT) is one of the most common disorders of the shoulder, especially in the middle-aged and elderly population. Yamamoto et al. (2010) reported that the prevalence of RCT was 20.7% and increased with age (Minagawa et al., 2013; Yamamoto

et al., 2010). The supraspinatus (SSP) is one of the four components of the rotator cuff, and this muscle is most affected by age-associated degenerative changes (Nobuhara, 2003) due to the mechanical stress under the acromion and the low blood flow around the SSP tendon. The treatment for RCT patients is applied physical therapy. As the rehabilitation therapy for RCT patients requires accurate evaluation

This is an open access article under the terms of the Creative Commons Attribution-NonCommercial License, which permits use, distribution and reproduction in any medium, provided the original work is properly cited and is not used for commercial purposes.

© 2021 The Authors. *Clinical Anatomy* published by Wiley Periodicals LLC on behalf of American Association of Clinical Anatomists.

and treatment of the SSP muscle dysfunction, it is important to understand the details of the SSP muscle function.

The SSP muscle in healthy individuals produces shoulder abduction torque in the scapular and coronal planes and acts to pull the humerus head into the glenoid fossa (Ackland et al., 2008; Alpert et al., 2000; Graichen et al., 2000; Hughes & An, 1996; Liu et al., 1997; Otis et al., 1994). RCT patients, on the other hand, experience SSP muscle atrophy (Hata et al., 2005; Kim et al., 2013; Meyer et al., 2005; Thomazeau et al., 1996). Kim et al. (2013) showed that the pennation angle of the SSP muscle was significantly smaller in RCT patients than in healthy individuals under relaxed and contracted conditions. The decrease in the pennation angle might be associated with muscle atrophy. Therefore, the SSP muscle in RCT patients might produce a lower shoulder abduction torque in the scapular plane due to SSP muscle atrophy as well as torn SSP muscle and tendon unit junction. However, the effect of RCT on the shoulder abduction torque in the scapular plane produced by the SSP muscle remains unclear. The SSP muscle is divided into anterior and posterior regions, and these regions have different architectures (Kim et al., 2007, 2010). Kim et al. (2007, 2010) demonstrated that the SSP muscle volume and fiber bundle length in the anterior region were larger than those in the posterior region. Therefore, the SSP muscle of the anterior region contributes more toward generating an active stiffness and pulling the humerus head into the glenoid fossa than the SSP muscle of the posterior region (Kim et al., 2010). Thus, different regions of the SSP muscle might contribute variably to the shoulder abduction in the scapular plane.

The functional characteristics of the SSP muscle have been examined in previous studies mainly using electromyography (EMG) (Alpert et al., 2000; Hawkes et al., 2012; Inman et al., 1996; Kronberg et al., 1990; Sakaki et al., 2013). As the measurements are performed using intramuscular fine-wire electrodes, the number of motor units that can be assessed in the same muscle is limited. As a result, the integrated value of EMG may not accurately reflect the true activity of the muscle region. Furthermore, the penetration of the wire electrode, though very localized, is invasive to the skin and muscles (Basmajian & Luca, 1985). In addition, pain is induced when the cathelin needle penetrates the skin. Therefore, the electromyographic method has limited value in estimating the active stiffness of each SSP muscle region *in vivo*.

On the other hand, previous studies suggest that the active stiffness of a muscle can be estimated using ultrasound shear-wave elastography (SWE). Bouillard et al. (2011) showed that the muscle stiffness more accurately estimates muscle force than muscle activity. More importantly, the evaluation method is painless and non-invasive. Hence, the evaluation of muscle stiffness during joint movement may be more useful in estimating the muscle force rather than the EMG. SWE has been reported as an effective evaluation method of skeletal muscle stiffness (Bouillard et al., 2011). As the muscle stiffness measured by SWE has a very high correlation with the muscle force in the dorsal interosseous muscle, abductor digiti minimi, biceps brachii, and tibialis anterior, SWE is effective in the evaluation of force exertion (Bouillard et al., 2011; Lacourpaille et al., 2012; Yoshitake

et al., 2014). Additionally, recent studies have shown that the assessment of the SSP muscle using SWE has high intra-examiner reliability (Baumer & Davis, 2017; Hatta et al., 2015).

Therefore, it is possible to determine whether each region contributes to active stiffness during shoulder abduction in the scapular plane by examining the change in stiffness for each region of the SSP muscle using SWE.

This study aimed to compare the effect of upper loads on the stiffness of the SSP muscle regions during isometric shoulder abduction in the scapular plane in RCT patients and in healthy individuals.

The hypothesis is that the SSP muscle regions on the tear side may have reduced force transmission during the shoulder abduction in the scapular plane. Therefore, the change in SSP stiffness from the resting phase to muscle contraction is expected to be less on the affected side as compared with that on the unaffected side and in healthy individuals. Additionally, the SSP muscle of the anterior region is anticipated to have a greater change in stiffness from the resting phase to muscle contraction because it contributes more toward generating active stiffness than the SSP muscle of the posterior region.

2 | MATERIALS AND METHODS

2.1 | Participants

The study protocol was approved by the appropriate ethics committee boards. Informed consent was obtained from all participants. The sample size was analyzed using power analysis software (G* Power ver 3.1, Institute of Experimental Psychology, Heinrich Heine University). Thirteen male patients scheduled for arthroscopic rotator cuff repair and 13 healthy male individuals were recruited. Results of the calculation were effect size 0.4, significance level 0.05, and power 0.8. The required sample size was 9. The exclusion criteria for RCT cases included the following: (i) a history of surgery on the ipsilateral and contralateral shoulder joints; (ii) RCT in the contralateral shoulder joint; (iii) osteoarthritis changes in the shoulder joint; (iv) torn subscapularis muscle; (v) neuromuscular disease or rheumatism; (vi) contracture in the shoulder joint; and (vii) inability to perform 30° shoulder isometric abduction in the scapular plane. Exclusion criteria for the healthy adult men were (i) orthopedic and neurologic disease, and (ii) a history of upper limb complaints or other musculoskeletal problems.

An experienced physician made the diagnosis of RCT based on magnetic resonance imaging and arthroscopic findings and assessed the contralateral side using ultrasound to confirm the absence of RCT, pain, or restricted movement. The degree of atrophy and the amount of fatty degeneration in the SSP muscle bellies was assessed on sagittal T1 images and was graded from 0 to 4 using the Goutallier classification (Goutallier et al., 1994). RCT size was assessed based on the largest dimension and was graded as small (<1 cm), medium (1–3 cm), large (3–5 cm), or massive (≥ 5 cm) (Cofield et al., 2001). Four patients had small RCTs; nine patients had medium RCTs. Furthermore, three patients had superficial partial-thickness injury and ten patients had a

full-thickness injury. Eight patients were classified as Goutallier grade 0 and five patients as Goutallier grade 1. All patients with RCTs had chronic SSP tears only. The time from initial symptoms to imaging was 398.1 ± 546.9 days. RCT was on the dominant shoulder in 46.1% (6 of 13) of the patients. We measured the dominant shoulder in 53.8% (7 of 13) of healthy individuals. There was no difference in age, height, weight, or percentage of dominant shoulder measurement between the two groups.

2.2 | Experimental protocol

Each participant was seated with the elbow joint of the affected arm extended and the thumb pointing upward and in the direction of shoulder elevation. Movement tasks included 30° shoulder isometric abduction in the scapular plane and maximal voluntary isometric contraction (MVIC) of shoulder abduction in the scapular plane. We measured the MVIC to assess the maximum muscle strength during the movement task. For RCT patients, shoulders on both the affected and unaffected sides were measured. On the other hand, for healthy individuals, shoulders chosen to match the percentage of RCT patients' dominant hand measurements were measured.

The movement tasks included passive abduction, abduction with the half-weight of the upper limb (1/2-weight), and abduction with the full weight of the upper limb (full-weight). Each movement task was performed twice using a custom-made device (Uchida Systems Co., Ltd., Tokyo, Japan) (Figure 1) that could set the shoulder joint angle. The angle of the cuff was set to 30° in the scapular plane using a goniometer (Tokyo university type; Matsuyoshi & Co., Ltd.). A force sensor (Mobie MT-100; Sakai Medical Co., Ltd., Tokyo, Japan) attached to the cuff of the device measured the weight of the upper limb. The weight of the upper limb determined the weight obtained by the force sensor when the measurement-side upper limb was relaxed by aligning the center of the elbow joint with the force sensor at the center of the cuff (Figure 2) (Suzuki et al., 2000). As a result, the weight of the measurement-side upper limb was 9.1 ± 1.4 N and the 1/2-weight of the measurement-side upper limb was 4.6 ± 1.7 N. The weight of the measurement-side upper limb was measured during 30° shoulder isometric abduction in the scapular plane. The data obtained by the force sensor were displayed on the monitor in real-time, and the participants were instructed to adjust to the target weight by looking at the readouts from the monitor during the movement task. Each movement task was performed twice randomly, with at least 30 s of rest between the tasks to eliminate the effects of fatigue.

2.3 | INSTRUMENTATION

2.3.1 | Muscle stiffness

The stiffness of the SSP muscle was recorded using SWE (AixPlover ver. 6; MSK mode, SuperSonic Imagine Co., Ltd., Aix-en-Provence, France) with a linear array probe (50 mm, 4–15 MHz).

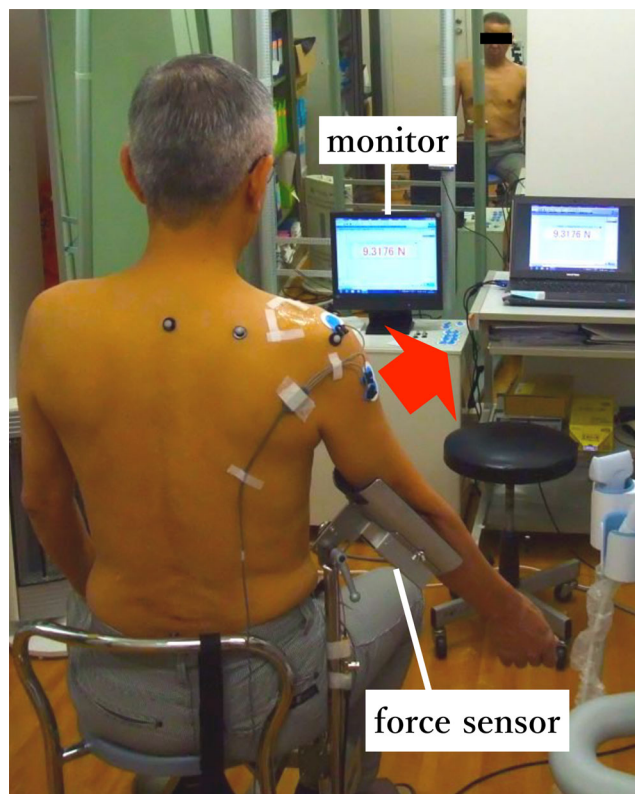


FIGURE 1 Measurement position. Participants were seated with their elbow joint extended and thumb pointed in the direction of vertical shoulder elevation. Each exercise task was performed using a custom-made device. The data obtained by the force sensor were displayed on a monitor in real-time, where the participant could visually confirm the load

The SSP muscle was divided into four regions according to muscle fiber orientation [anterior superficial (AS), anterior deep (AD), posterior superficial (PS), and posterior deep (PD) regions] (Hatta et al., 2015; Itoigawa et al., 2015) (Figure 3). The location of the probe was marked with permanent ink after securing the clearest image (Taniguchi et al., 2015). The muscle stiffness was also measured. An acoustic gel was used as an interface between the probe and skin for all imaging, with the probe being held gently over the skin without pressure on the tissues underneath (Taniguchi et al., 2015).

The stiffness data of the SSP muscles were calculated using an analysis program (Q-Box) installed in the SWE system. Local shear-wave propagation velocity (c) distribution in the longitudinal direction of the muscle was visualized at 1 Hz as a color-coded map (1×1 mm² spatial resolution) superimposed on the longitudinal B-mode image. For each region of interest (ROI; 15×15 mm² in each muscle fascicular area), Young's modulus (E) was calculated as $E = 3qc^2$, where the density (q) was assumed to be constant (1000 kg/m³) in human soft tissues. A larger shear-wave velocity (SWV) indicated greater Young's modulus and stiffness (Ates et al., 2015; Yavuz et al., 2015). Within the ROI, three circular areas (diameter 3–7 mm), which encompassed each

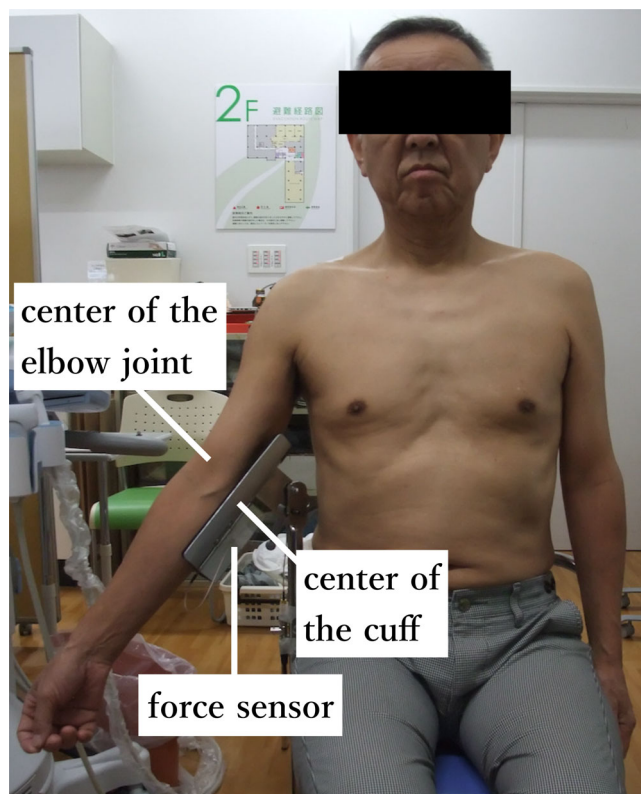
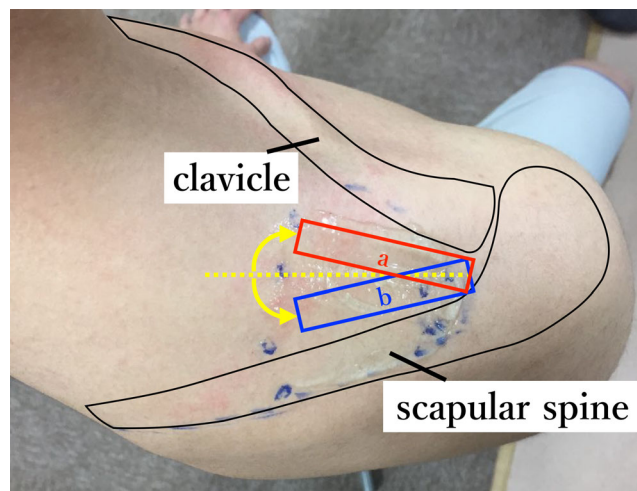


FIGURE 2 A force sensor attached to the cuff. A force sensor attached to the cuff of the device measured the weight of the upper limb. The weight of the upper limb determined the weight obtained by the force sensor when the measurement-side upper limb was relaxed by aligning the center of the elbow joint with the force sensor at the center of the cuff

muscle region, were selected (Figure 4). The SWV in the selected circular areas (in m/s) was calculated using Q-Box. The mean value of the two measurements for each muscle region was used for the statistical analyses.

2.3.2 | Electromyography

We expected muscle activation to be absent during the passive movement task. In order to corroborate this expected finding, electrodes were placed in the middle deltoid (MD) muscle to obtain EMG signals for muscle activity. The MD muscle was reported to contribute to shoulder abduction in the scapular plane (Ackland et al., 2008; Alpert et al., 2000; Liu et al., 1997); therefore, we selected it as a test muscle. EMG signals from the MD muscle were recorded using active surface electrodes. The electrodes were placed on the intersection of the center of the anterior deltoid muscle and the posterior deltoid muscle and the intersection of the center of the acromion and the deltoid tuberosity in the shoulder neutral position (Sakaki et al., 2013). Electrode specifications used in this study were as follows: frequency response, 5–500 Hz; amplification, differential; inter-electrode distance, 12 mm; contact sensors, two 10×6 mm silver bars; preamplifier gain,



a: Anterior region b: Posterior region

FIGURE 3 Probe position. The ultrasound probe was first placed perpendicularly to the skin surface in the middle of the spine of the scapula, in the mediolateral direction, and between the clavicle and scapular spine in the anteroposterior direction to identify the proper orientation of the intramuscular tendon (start position). The probe was then rotated either clockwise (a) or counter-clockwise (b) from the start position until the muscle region displayed in the B-mode ultrasound screen reached its maximal length. When the shear-wave elastography images were collected in each quadrant, the orientation of the probe was fine-tuned by inclining it sagittally within $\pm 20^\circ$ until the muscle fiber length in the B-mode image of that quadrant was maximal

500-fold; input impedance, $>200 \text{ M}\Omega$; and common-mode rejection ratio, $>110 \text{ dB}$. The signals from the EMG system were sampled at 2000 Hz using an analog-to-digital converter (Power Lab; AD Instruments Co., Ltd., Melbourne, Victoria, Australia) and stored on a personal computer using Chart 5.3 software (LabChartTM ver. 7; AD Instruments Co., Ltd., Melbourne, Victoria, Australia) (Kato et al., 2019).

First, the electrode attachment site on the MD muscle was identified. Next, prior to attachment, the skin was shaved, abraded, and cleaned with alcohol. The skin surface was also polished with a skin pretreatment agent for stable electrode contact (Skin Pure; Nihon Kohden Co., Ltd., Tokyo, Japan). Next, participants performed shoulder abduction movement in the sitting position to record MVIC of the MD muscle. The participant was instructed to produce muscular contraction gradually in 2 s, sustained MVIC for 5 s, and then relax gradually for 2 s. The MVIC was recorded after a total of two MVICs were performed.

The EMG signals were high-pass filtered at a cutoff frequency of 20 Hz (Kato et al., 2019) and full wave-rectified. To calculate the root mean square (RMS) during each trial, the data of each trial were standardized as the average value for 1 s with the MVIC as 100% (%RMS). The trials in which the EMG data exceeded $>2\%$ or more of the MVIC were excluded from the analysis (Le Sant et al., 2015).

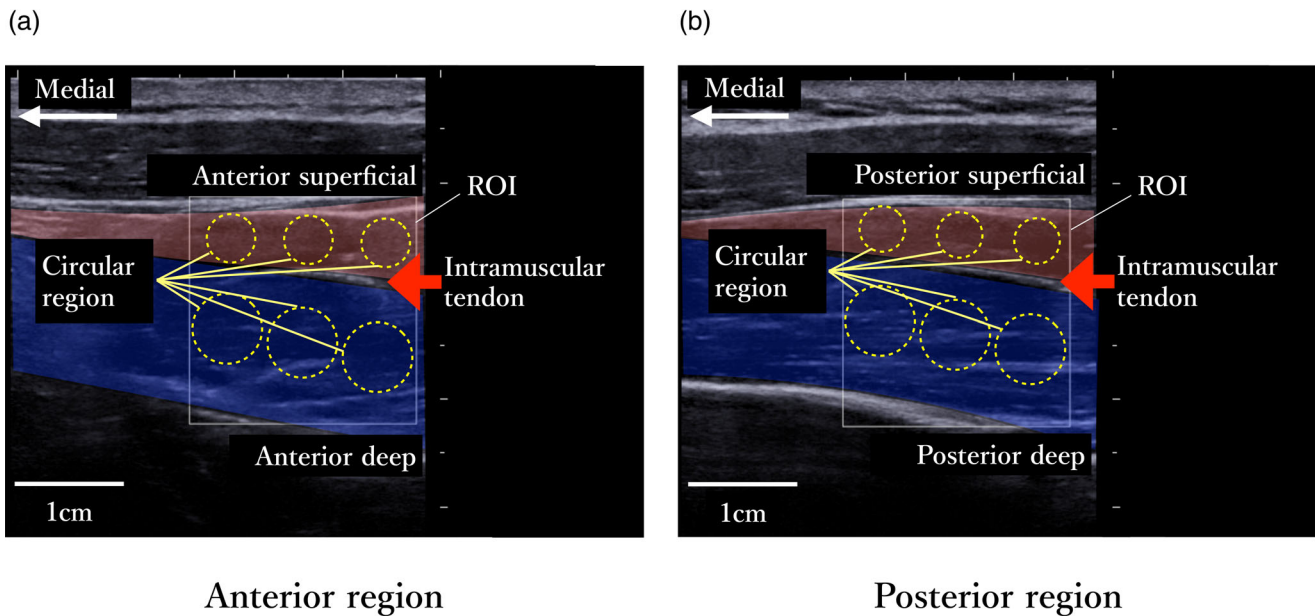


FIGURE 4 Analysis of images of the supraspinatus (SSP) muscle. The left and right figures show a B-mode image for the anterior (a) and posterior (b) regions of the SSP muscle, respectively. The anterior and posterior regions were further divided into superficial (pink) and deep (blue) regions bounded by the intramuscular tendon, with the superficial region being the one superior to the intramuscular tendon and the deep region inferior to it. Within the above region of interest (ROI), three circular areas of 3–7 mm in diameter, which encompassed each muscle region, were selected

2.3.3 | Muscle strength

The maximum shoulder abduction strength in the scapular plane was measured to determine the maximum muscle strength during the movement task. We measured muscle strength in order to quantify the loss of muscle function due to RCT, and also for its strong correlation to active stiffness (Bouillard et al., 2011). Muscle strength was measured during the 30° shoulder isometric abduction in the scapular plane and recorded using a force sensor (Mobie MT-100; Sakai Medical Co., Ltd., Tokyo, Japan). We measured muscle strength simultaneously with muscle activity. The mean of the two muscle strength measurements was used for statistical analysis.

2.4 | Statistical analysis

All statistical analyses were performed using IBM SPSS Statistics for Windows, version 21.0 (SPSS Inc., Chicago, IL, USA). The repeatability of shear modulus measurements within a session was examined using the intraclass correlation coefficient (ICC). Repeatability was assumed to be good if ICC > 0.75, moderate if ICC was 0.50–0.75, and poor if ICC < 0.50, using previously established criteria (Portney & Watkins, 2019). Non-parametric tests were used in this study because the stiffness data of each muscle region and muscle strength were partially non-normally distributed, and the sample size was not large. The Mann–Whitney test was used to compare the age, height, and weight in each group. Further, the chi-square test was used to assess the percentage of the dominant

shoulder side. Friedman with Dunn's post hoc test was used to compare the SWV of each muscle region and MVIC between groups (Hatta et al., 2016; Kato et al., 2021). The level of significance was set at 5% for all tests, and data are presented as mean and standard deviation in the text and mean and standard error in the figures.

3 | RESULTS

Participants were recruited from November 14 to December 1, 2017. In expectation of losses to follow-up, we recruited 26 participants in total. Three of the RCT patients were excluded from the analysis because one patient had a torn subscapularis muscle and two patients could not perform 30° shoulder isometric abduction in the scapular plane. As a result, we analyzed 10 RCT patients (age: 62.6 ± 9.0 years, height: 165.9 ± 6.6 cm, body mass: 68.3 ± 7.6 kg) and 13 healthy individuals (age: 55.9 ± 8.8 years, height: 169.2 ± 6.8 cm, body mass: 68.1 ± 6.4 kg).

3.1 | Intraclass correlation coefficient, muscle activity, muscle strength

Good intrasession reliability (ICC > 0.75) was found for the shear modulus measured in the anterior region of the SSP muscle [ICC = 0.98, 95% confidence interval (CI): 0.93–0.99] and the posterior region of the SSP muscle (ICC = 0.98, 95% CI: 0.94–0.99).

The %RMS of the affected MD muscle was $1.3\% \pm 0.1\%$ and that of the unaffected and control MD muscle was $1.0\% \pm 0.1\%$.

Muscle strength on the affected side was significantly lower than that on the control side (control: 332.94 ± 186.08 Nm; affected: 126.46 ± 68.89 Nm; $p = 0.04$) (Figure 5).

3.2 | Shear-wave velocity

The SWV of the AS on the affected side was significantly lower than that on the control side during the 1/2-weight (control: 4.05 ± 1.10 m/s; affected: 2.64 ± 1.17 m/s; $p = 0.04$) and full-weight tasks (control: 4.60 ± 1.13 m/s; affected: 2.70 ± 1.18 m/s; $p = 0.04$) (Figure 6a). Additionally, there was no significant difference in the SWV of AS during the passive movement task. There was no significant difference in the SWV of all regions between the unaffected sides and controls in all tasks.

There was no significant difference in the SWV of the AD, PS, and PD between groups (Figures 6b and 7).

4 | DISCUSSION

In this study, we showed that in comparison to the AS on the control side, the SWV of the AS on the affected side was 1.41 m/s (34.72%) and 1.90 m/s (41.27%) lower for the 1/2-weight task and full-weight task, respectively. While several previous studies reported a change in stiffness during passive shoulder joint movement in cadavers, RCT patients, and healthy participants (Baumer & Dischler, 2017; Hatta et al., 2015; Itoigawa et al., 2015), few studies have examined the stiffness of the SSP muscle during active shoulder joint movement in RCT patients (Baumer & Dischler, 2017). Furthermore, to the best of our knowledge, this is the first study that investigated the mechanical effects of different loads on different regions of the SSP muscle in RCT patients.

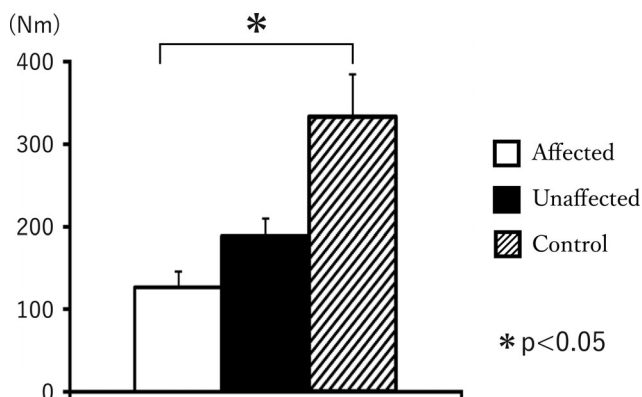


FIGURE 5 The maximum shoulder abduction strength in the scapular plane. The muscle strength on the affected side was significantly lower than that on the control side

The reproducibility of the shear modulus measurements in the SSP muscle was good; the ICC was well above 0.75 (0.93–0.99). The reliability of the SSP muscle measurements using SWE had been investigated in several studies (Baumer & Davis, 2017; Hatta et al., 2015). Hatta et al. (2015) demonstrated that all the regions of the SSP muscle in vitro had high measurement reliability, with the intra-observer ICC values of >0.83 . Moreover, Baumer & Davis (2017) showed that SWE imaging of the SSP muscle in vivo had high reliability, with intra-observer ICC values of >0.99 . Collectively, the reproducibility of the present shear modulus measurements performed in our study was consistent with most of the current literature.

The %RMS of MD muscle during the passive movement task was approximately 1.0% on the affected, unaffected, and control sides. Our %RMS values were below the 2% reported in a previous study (Le Sant et al., 2015). While the previous study (Le Sant et al., 2015) recruited healthy subjects, our study recruited RCT patients. The %RMS could exceed 2% as the RCT patients did not demonstrate MVIC. It was, therefore, recognized that the MD muscle activity was barely significant during the passive movement task.

The maximum shoulder abduction strength in the scapular plane on the affected side was 206.49 Nm (62.02%), lower than that on the control side. In addition, our results indicate that mainly the active stiffness of the affected AS decreased compared with that of other SSP muscle regions. Mendias et al. (2015) identified that the SSP muscle in patients with RCT had a striking deficit specifically in the force production of the residual muscle fibers, structural abnormalities in the architecture of muscle contractile proteins and abnormalities in the shape of mitochondria surrounding lipid droplets. Moreover, Ward et al. (2010) reported that the muscle mass and length were lower, sarcomere length was shorter, and sarcomere number was reduced in the rat model of the SSP tear. Regarding the muscle fiber-specific characteristics of the SSP muscle, Kim et al. (2007, 2010) suggested that the SSP muscle of the anterior region contributed more toward generating active stiffness and pulling the humerus head into the glenoid fossa than the SSP muscle of the posterior region. Furthermore, Meyer et al. (2005) showed that the superficial region of the SSP muscle contributed far more to muscle atrophy than the deep region. Therefore, the AS in RCT is primarily responsible for the reduced active stiffness because the AS contributes to the production of the shoulder abduction torque in the scapular plane, and the AS in RCT undergoes greater atrophy in comparison to other SSP muscle regions.

The present SWE results indicate that the active stiffness of the AS decreased more than that of the other SSP muscle regions in the RCT patients. Therefore, it is important to avoid overloading the AS; instead, the focus should be shifted to strengthening the other rotator cuff and shoulder muscles. To construct a physical therapy program for each SSP muscle region, however, it is necessary to investigate the active stiffness of each SSP muscle region during various movement tasks.

This study has three main limitations. First, the location and size of the RCT differed between patients; thus, the real-life results may deviate from the findings derived from this study depending on the

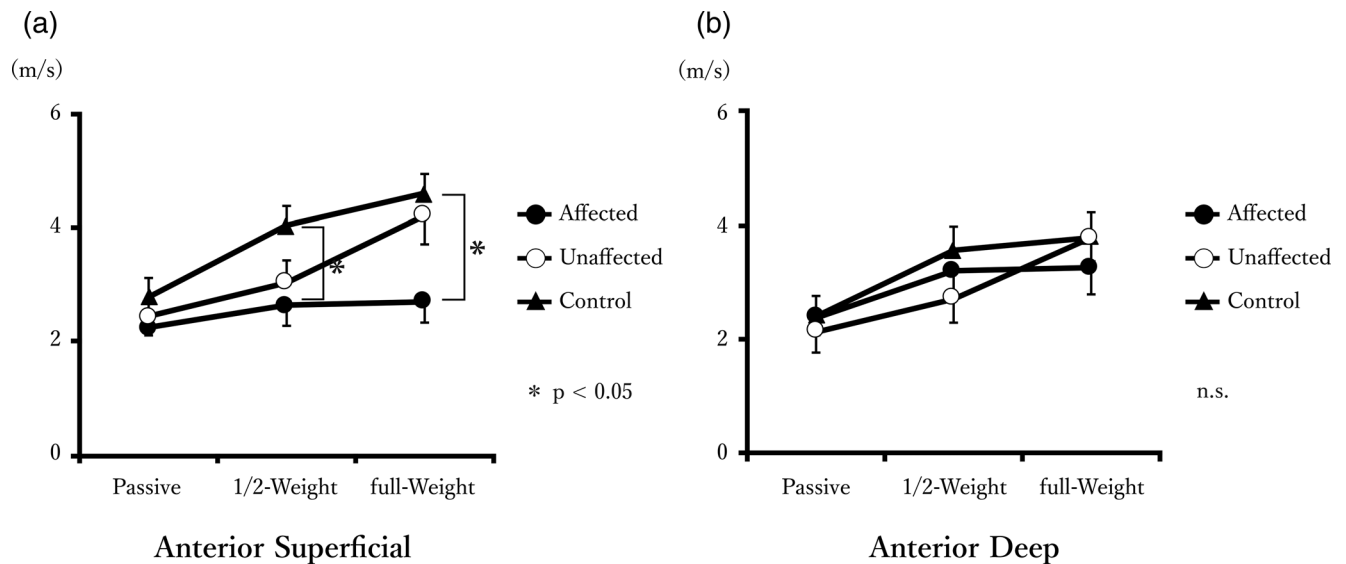


FIGURE 6 Shear wave velocity (SWV) for the anterior superficial (a) and deep (b) regions of the supraspinatus (SSP) muscle. The left and right graphs show the SWV for the anterior superficial (AS) (A) and anterior deep (AD) (B) regions of the SSP muscle, respectively. The SWV of the AS on the affected side was significantly lower than that of AS on the control side during the 1/2-weight and full-weight tasks. Additionally, there was no significant difference in the SWV of AS during the passive movement task. There was no significant difference in the SWV of the AD. n.s., not significant

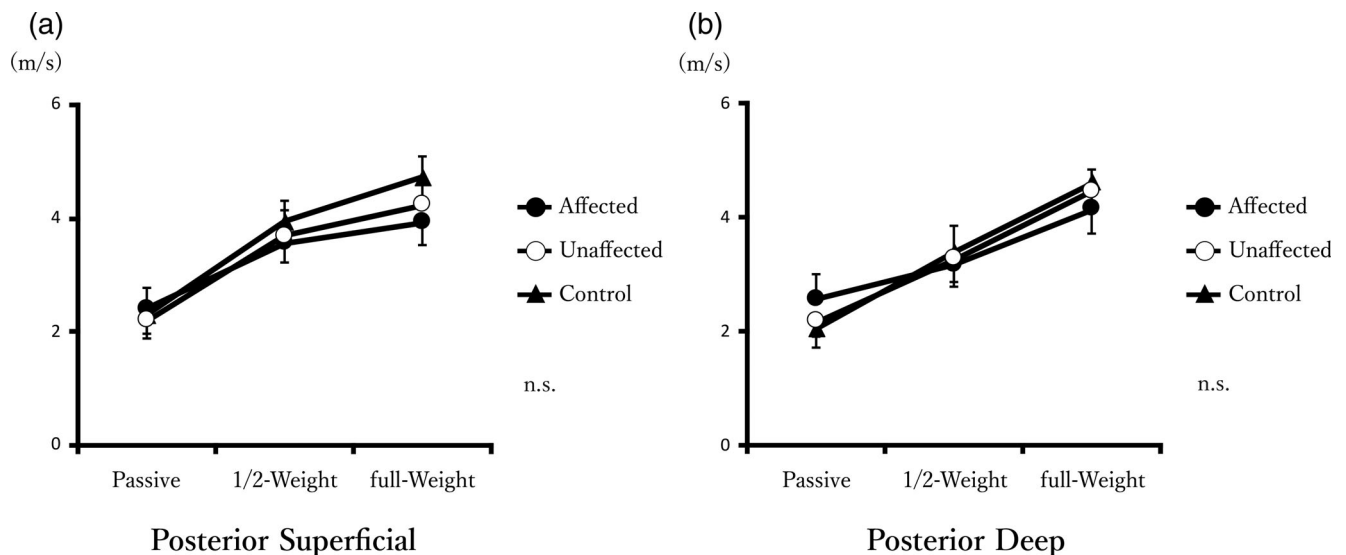


FIGURE 7 Shear wave velocity (SWV) for the posterior superficial (a) and deep (b) regions of supraspinatus (SSP) muscle. The left and right graphs show the SWV of the posterior superficial (PS) (a) and posterior deep (PD) (b) regions of the SSP muscle, respectively. There was no significant difference in the SWV of the PS and PD. n.s., not significant

tear position, tear size, tear morphology, and continuity of the muscle-tendon tissue. It is, therefore, necessary to investigate the effects of the structure of the SSP tendon on muscle stiffness in the future. Second, the measurements were performed in only one limb position. In this study, the stiffness was measured by 30° shoulder isometric abduction in the scapular plane, which is frequently used for the evaluation and treatment of the SSP muscle. We could perform measurements with almost no pain because the measurement position in the scapular plane is the more comfortable limb position. However, the

shoulder joint is a free joint, and it is assumed that the SSP muscle contributes to other movement directions. For future studies, it will be necessary to measure the changes in the stiffness of the SSP muscle as applied to other directions of shoulder movement. Third, the direct relationship between the change in stiffness of the SSP muscle and the active stiffness of the SSP muscle has not been explored. The relationship between the active stiffness and elasticity has been proven for the biceps brachii muscle, which is near the shoulder joint, as well as the dorsal interosseous and tibialis anterior muscles, which

are the pennate muscles similar to the SSP muscle (Bouillard et al., 2011; Lacourpaille et al., 2012; Yoshitake et al., 2014). Therefore, it is reasonable to evaluate the force exertion of the SSP muscle, which has similar muscle morphology and high intra-observer reliability. The stiffness of the SSP muscle has been examined in recent years (Baumer & Dischler, 2017; Ishikawa et al., 2015). In the future, it will be necessary to verify the direct relationship between the change in stiffness of the SSP muscle and the active force of the SSP muscle.

In conclusion, the SWV of the AS on the affected side was significantly lower than that on the control side during the 1/2-weight and full-weight tasks. Based on our findings, the active stiffness of the AS in RCT may be primarily reduced during the isometric shoulder abduction in the scapular plane. Hence, the AS should be the focal point when quantitatively evaluating the dysfunction of the SSP muscle in the case of RCT. In the future, it will be necessary to study the active stiffness of each SSP muscle region during various movement tasks to construct appropriate physical therapy treatment programs.

ACKNOWLEDGMENTS

We would like to thank the staff of Hitsujigaoka Hospital and the Sports Physical Therapy Laboratory at Sapporo Medical University. This study was supported by a Grant-in-Aid for Early Career Scientists (19K19833).

ORCID

Yoshinari Sakaki  <https://orcid.org/0000-0003-1280-3583>

REFERENCES

- Ackland, D. C., Pak, P., Richardson, M., & Pandy, M. G. (2008). Moment arms of the muscles crossing the anatomical shoulder. *Journal of Anatomy*, 213(4), 383–390.
- Alpert, S. W., Pink, M. M., Jobe, F. W., McMahon, P. J., & Mathiyakom, W. (2000). Electromyographic analysis of deltoid and rotator cuff function under varying loads and speeds. *Journal of Shoulder and Elbow Surgery*, 9(1), 47–58.
- Ates, F., Hug, F., Bouillard, K., Jubeau, M., Frappart, T., Couade, M., Bercoff, J., & Nordez, A. (2015). Muscle shear elastic modulus is linearly related to muscle torque over the entire range of isometric contraction intensity. *Journal of Electromyography and Kinesiology*, 25(4), 703–708.
- Basmajian, J. V., & Luca, C. J. D. (1985). *Muscles alive: Their functions revealed by electromyography* (5th ed.). Baltimore: Williams & Wilkins.
- Baumer, T. G., Davis, L., Dischler, J., Siegal, D. S., van Holsbeeck, M., Moutzouros, V., & Bey, M. J. (2017). Shear wave elastography of the supraspinatus muscle and tendon: Repeatability and preliminary findings. *Journal of Biomechanics*, 28(53), 201–204.
- Baumer, T. G., Dischler, J., Davis, L., Labyed, Y., Siegal, D. S., van Holsbeeck, M., Moutzouros, V., & Bey, M. J. (2017). Effects of age and pathology on shear wave speed of the human rotator cuff. *Journal of Orthopaedic Research*, 36(1), 282–288.
- Bouillard, K., Nordez, A., & Hug, F. (2011). Estimation of individual muscle force using elastography. *PLoS One*, 6(12), e29261.
- Cofield, R. H., Parvizi, J., Hoffmeyer, P. J., Lanzer, W. L., Ilstrup, D. M., & Rowland, C. M. (2001). Surgical repair of chronic rotator cuff tears. A prospective long-term study. *The Journal of Bone and Joint Surgery. American Volume*, 83-A(1), 71–77.
- Goutallier, D., Postel, J. M., Bernageau, J., Lavau, L., & Voisin, M. C. (1994). Fatty muscle degeneration in cuff ruptures. Pre- and postoperative evaluation by CT scan. *Clinical Orthopaedics and Related Research*, 304, 78–83.
- Graichen, H., Stammberger, T., Bonel, H., Englmeier, K. H., Reiser, M., & Eckstein, F. (2000). Glenohumeral translation during active and passive elevation of the shoulder—A 3D open-MRI study. *Journal of Biomechanics*, 33(5), 609–613.
- Hata, Y., Saitoh, S., Murakami, N., Kobayashi, H., Kaito, T., & Kato, H. (2005). Volume changes of supraspinatus and infraspinatus muscles after supraspinatus tendon repair: A magnetic resonance imaging study. *Journal of Shoulder and Elbow Surgery*, 14(6), 631–635.
- Hatta, T., Giambini, H., Hooke, A. W., Zhao, C., Sperling, J. W., Steinmann, S. P., Yamamoto, N., Itoi, E., & An, K. N. (2016). Comparison of passive stiffness changes in the supraspinatus muscle after double-row and knotless transosseous-equivalent rotator cuff repair techniques: A cadaveric study. *Arthroscopy*, 32(10), 1973–1981.
- Hatta, T., Giambini, H., Uehara, K., Okamoto, S., Chen, S., Sperling, J. W., Itoi, E., & An, K. N. (2015). Quantitative assessment of rotator cuff muscle elasticity: Reliability and feasibility of shear wave elastography. *Journal of Biomechanics*, 48(14), 3853–3858.
- Hawkes, D. H., Alizadehkhayat, O., Kemp, G. J., Fisher, A. C., Roebuck, M. M., & Frostick, S. P. (2012). Shoulder muscle activation and coordination in patients with a massive rotator cuff tear: An electromyographic study. *Journal of Orthopaedic Research*, 30(7), 1140–1146.
- Hughes, R. E., & An, K. N. (1996). Force analysis of rotator cuff muscles. *Clinical Orthopaedics and Related Research*, 330, 75–83.
- Inman, V. T., Saunders, J. B., & Abbott, L. C. (1996). Observations of the function of the shoulder joint. *Clinical Orthopaedics and Related Research*, 330, 3–12.
- Ishikawa, H., Muraki, T., Sekiguchi, Y., Ishijima, T., Morise, S., Yamamoto, N., Itoi, E., & Izumi, S.-I. (2015). Noninvasive assessment of the activity of the shoulder girdle muscles using ultrasound real-time tissue elastography. *Journal of Electromyography and Kinesiology*, 25(5), 723–730.
- Itoigawa, Y., Sperling, J. W., Steinmann, S. P., Chen, Q., Song, P., Chen, S., Song, P., Chen, S., Itoi, E., Hatta, T., & An, K. N. (2015). Feasibility assessment of shear wave elastography to rotator cuff muscle. *Clinical Anatomy*, 28(2), 213–218.
- Kato, T., Taniguchi, K., Akima, H., Watanabe, K., Ikeda, Y., & Katayose, M. (2019). Effect of hip angle on neuromuscular activation of the adductor longus and adductor magnus muscles during isometric hip flexion and extension. *European Journal of Applied Physiology*, 119(7), 1611–1617.
- Kato, T., Taniguchi, K., Kikukawa, D., Kodesho, T., & Katayose, M. (2021). Effect of hip flexion angle on stiffness of the adductor longus muscle during isometric hip flexion. *Journal of Electromyography and Kinesiology*, 56, 102493.
- Kim, S. Y., Bleakney, R., Boynton, E., Ravichandiran, K., Rindlisbacher, T., McKee, N., & Agur, A. (2010). Investigation of the static and dynamic musculotendinous architecture of supraspinatus. *Clinical Anatomy*, 23(1), 48–55.
- Kim, S. Y., Bleakney, R. R., Rindlisbacher, T., Ravichandiran, K., Rosser, B. W., & Boynton, E. (2013). Musculotendinous architecture of pathological supraspinatus: A pilot in vivo ultrasonography study. *Clinical Anatomy*, 26(2), 228–235.
- Kim, S. Y., Boynton, E. L., Ravichandiran, K., Fung, L. Y., Bleakney, R., & Agur, A. M. (2007). Three-dimensional study of the musculotendinous architecture of supraspinatus and its functional correlations. *Clinical Anatomy*, 20(6), 648–655.
- Kronberg, M., Nemeth, G., & Brostrom, L. A. (1990). Muscle activity and coordination in the normal shoulder. An electromyographic study. *Clinical Orthopaedics and Related Research*, 257, 76–85.
- Lacourpaille, L., Hug, F., Bouillard, K., Hogrel, J. Y., & Nordez, A. (2012). Supersonic shear imaging provides a reliable measurement of resting

- muscle shear elastic modulus. *Physiological Measurement*, 33(3), N19–N28.
- Le Sant, G., Ates, F., Brasseur, J. L., & Nordez, A. (2015). Elastography study of hamstring behaviors during passive stretching. *PLoS One*, 10(9), e0139272.
- Liu, J., Hughes, R. E., Smutz, W. P., Niebur, G., & Nan-An, K. (1997). Roles of deltoid and rotator cuff muscles in shoulder elevation. *Clinical Biomechanics (Bristol, Avon)*, 12(1), 32–38.
- Mendias, C. L., Roche, S. M., Harning, J. A., Davis, M. E., Lynch, E. B., Sibilsy Enselman, E. R., Jacobson, J. A., Clafin, D. R., Calve, S., & Bedi, A. (2015). Reduced muscle fiber force production and disrupted myofibril architecture in patients with chronic rotator cuff tears. *Journal of Shoulder and Elbow Surgery*, 24(1), 111–119.
- Meyer, D. C., Pirkel, C., Pfirrmann, C. W. A., Zanetti, M., & Gerber, C. (2005). Asymmetric atrophy of the supraspinatus muscle following tendon tear. *Journal of Orthopaedic Research*, 23(2), 254–258.
- Minagawa, H., Yamamoto, N., Abe, H., Fukuda, M., Seki, N., Kikuchi, K., Kijima, H., & Itoi, E. (2013). Prevalence of symptomatic and asymptomatic rotator cuff tears in the general population: From mass-screening in one village. *Journal of Orthopaedics*, 10(1), 8–12.
- Nobuhara, K. (2003). *The shoulder: Its function and clinical aspects* (1st ed.). River Edge: World Scientific Publishing Co Pvt Ltd.
- Otis, J. C., Jiang, C. C., Wickiewicz, T. L., Peterson, M. G., Warren, R. F., & Santner, T. J. (1994). Changes in the moment arms of the rotator cuff and deltoid muscles with abduction and rotation. *The Journal of Bone and Joint Surgery*, 76(5), 667–676.
- Portney, L. G., & Watkins, M. P. (2019). *Foundations of clinical research: Applications to practice* (4th ed). Philadelphia: F.A. Davis Co.
- Sakaki, Y., Kaneko, F., Watanabe, K., Kobayashi, T., Katayose, M., Aoki, N., Shibata, E., & Yamashita, T. (2013). Effects of different movement directions on electromyography recorded from the shoulder muscles while passing the target positions. *Journal of Electromyography and Kinesiology*, 23(6), 1362–1369.
- Suzuki, N., Kizuka, T., Noguchi, H., Tanaka, S., Shimojo, H., Shiraki, H., Mukai, N., & Miyanaga, Y. (2000). Electromyographic analysis of shoulder muscles during shoulder external rotation with reference to load magnitude. *The Journal of Physical Fitness and Sports Medicine*, 49(4), 481–494.
- Taniguchi, K., Shinohara, M., Nozaki, S., & Katayose, M. (2015). Acute decrease in the stiffness of resting muscle belly due to static stretching. *Scandinavian Journal of Medicine & Science in Sports*, 25(1), 32–40.
- Thomazeau, H., Rolland, Y., Lucas, C., Duval, J. M., & Langlais, F. (1996). Atrophy of the supraspinatus belly. Assessment by MRI in 55 patients with rotator cuff pathology. *Acta Orthopaedica Scandinavica*, 67(3), 264–268.
- Ward, S. R., Sarver, J. J., Eng, C. M., Kwan, A., Wurgler-Hauri, C. C., Perry, S. M., Williams, G. R., Soslowsky, L. J., & Lieber, R. L. (2010). Plasticity of muscle architecture after supraspinatus tears. *The Journal of Orthopaedic and Sports Physical Therapy*, 40(11), 729–735.
- Yamamoto, A., Takagishi, K., Osawa, T., Yanagawa, T., Nakajima, D., Shitara, H., & Kobayashi, T. (2010). Prevalence and risk factors of a rotator cuff tear in the general population. *Journal of Shoulder and Elbow Surgery*, 19(1), 116–120.
- Yavuz, A., Bora, A., Bulut, M. D., Batur, A., Milanlioglu, A., Goya, C., & Andic, C. (2015). Acoustic radiation force impulse (ARFI) elastography quantification of muscle stiffness over a course of gradual isometric contractions: A preliminary study. *Medical Ultrasonography*, 17(1), 49–57.
- Yoshitake, Y., Takai, Y., Kanehisa, H., & Shinohara, M. (2014). Muscle shear modulus measured with ultrasound shear-wave elastography across a wide range of contraction intensity. *Muscle & Nerve*, 50(1), 103–113.

How to cite this article: Sakaki, Y., Taniguchi, K., Katayose, M., Kura, H., & Okamura, K. (2022). Effects of shoulder abduction on the stiffness of supraspinatus muscle regions in rotator cuff tear. *Clinical Anatomy*, 35(1), 94–102. <https://doi.org/10.1002/ca.23800>